

PAPER REF: 6974

EXPERIMENTAL AND CALCULATED STUDY OF DYNAMIC CHARACTERISTICS OF WATER-SATURATED SAND

Anatoly Bragov^(*), Vladimir Balandin, Vasily Kotov

Research Institute of Mechanical, Lobachevsky State University, Nizhny Novgorod, Russia

^(*)*Email:* bragov@mech.unn.ru

ABSTRACT

The study of physical and mechanical properties of soils under dynamic loading is carried out for a long time. This paper presents the results of reversed ballistic experiments with targets of dry and water saturated sand and the results of calculations. The flat end of measuring rod was used as a projectile. From the calculations, it follows that there is almost complete water saturation of compacted sand its shear properties are reduced, however, they are essential and need to be considered when assessing the penetration resistance of solids into the water saturated sand.

Keywords: dry and water saturated sand, reversed ballistic experiment, shear properties, penetration resistance

INTRODUCTION

Physical-mechanical characteristics of sandy soils under dynamic loading have been studied long enough (Omidvar, 2012). The developed plane-wave experiment methodologies make it possible to determine the shock adiabat of dry and wet sand in the loading range of up to several GPa (Dianov,1977; Bragov,1993; Arlery, 2010), whereas shear properties are determined experimentally, using the modified Kolsky methodology, for substantially lower pressures (Bragov,1996; Bragov,2004; Martin, 2009; Balandin, 2015a).

It is known that compaction of sand results in the changes of its strength properties, leading, for example, to substantially changing penetration depths of strikers. The inverse experiment methodology (Balandin, 2015a; Bragov,2006) makes it possible to determine both shock adiabats of dry sand with increased density, based on maximum values of the resistance force and quasi-stationary resistance forces (Balandin, 2016). It was shown earlier that shearing characteristics of soils correlate with the values of the resistance force at the quasi-stationary stage of penetration (Kotov, 2013; Bazhenov,2008; Bazhenov,2009).

The present paper presents the data of the laboratory studies of dynamic compressibility and shearing resistance of a sandy soil based on the experimental-computational analysis of the resistance force values at the quasi-stationary stage of the penetration of a cylindrical measuring rod striker with a flat end in the framework of the inverse experiment methodology. It is shown that shearing properties of a practically fully water-saturated sand degrade but remain substantial enough to be taken into account. The obtained results will be useful in analyzing applied problems of penetration of solids into soil media.

CHARACTERISTIC FEATURES OF DYNAMICALLY TESTING WATER-SATURATED SOILS IN THE INVERSE EXPERIMENT

Methodology of the Inverse Experiment

A simple and effective inverse experiment methodology for investigating dynamic properties of soft soils and other low-density media is described in detail in (Bragov,2006). The experimental set implementing this method is schematically presented in Fig. 1 (Balandin, 2016). In the present version of the inverse experiment, a container with soil is accelerated using a 57mm-dia gas gun (1) with a two-diaphragm breech block (2), providing stable and easily controlled impact velocities in the range of 50 to 500 m/s.

The container is a thin-walled cartridge of the D16-T aluminum alloy (3), filled with a soil medium (4). To prevent the soil from spilling in the course of preparing the experiment and during acceleration, the front part of the cartridge is sealed with 0,01mm-thick lavsan film (5). The film is secured and fitted to the soil surface with a vinyl-resin ring (6).

The impact velocity of the container was determined using two electric contact gages (7) situated in the holes in the barrel, drilled near its muzzle. A 1.5m-long 20mm-dia steel rod with the yield strength of over 2000 MPa was used as a force-measuring rod (8). One of the ends of the measuring rod has a threaded hole (M10) housing a threaded cylindrical striker of a required nose geometry (9). The rod is located at a distance from the barrel muzzle, so that the impact takes place as soon as the container completely leaves the barrel. The base supporting the rod is equipped with adjusting supports (10) which make it possible to provide an axisymmetric character of the interaction. The rear end of the rod rests against a special support (11) preventing its displacement and damping the impact energy. The impact takes place in a vacuum chamber (12), connected to the gun barrel (13), and housing measuring rod (8) with striker (9). The 19,8mm-dia striker heads with the hemisphere radius of 10mm were made of the 45 steel ($\sigma_T \geq 600$ MPa) and the EP638 steel ($\sigma_T \geq 1800$ MPa).

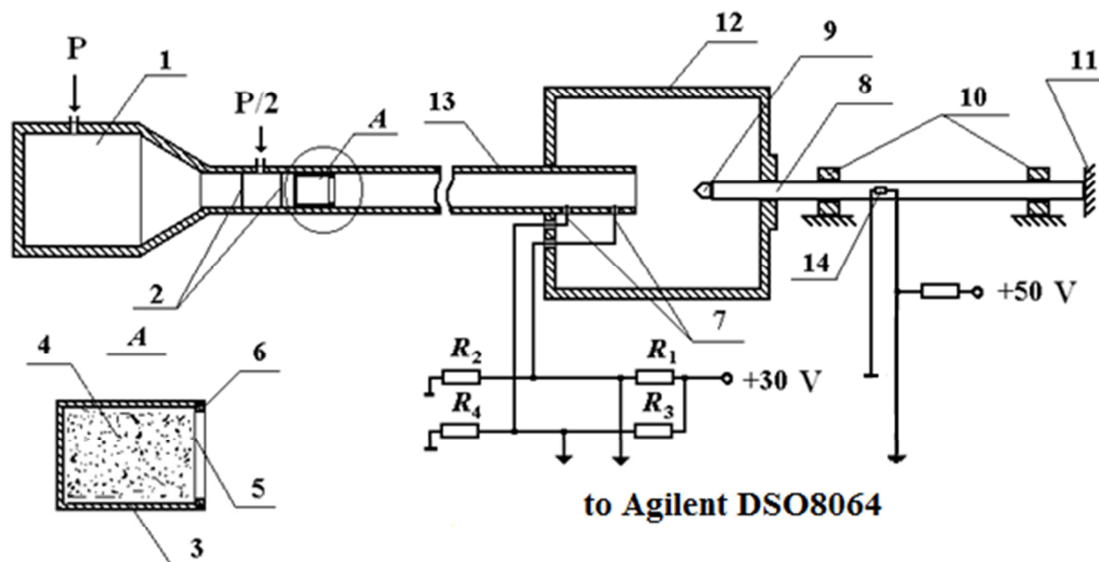


Fig.1. - Schematic view of the stand for measuring penetration resisting forces in the inverse experiment.

The soil-filled container is accelerated up to required velocities using the gas gun and hits the flat end of the measuring rod, in which elastic strain pulse $e(t)$ is formed. By registering this pulse on the surface of the measuring rod it is possible to evaluate force F , acting on the

striker interacting with the medium, using a known relation $F(t) = Ee(t)S_0$, where E is elastic modulus of the rod, S_0 is cross-section area. Using Hugoniot relations along the rod-soil interface, shock wave velocity D is found as a function of mass velocity u :

$$D(u) = F/(\rho_0 u S_0), \quad u = V_0 - F/(\rho c_0 S_0), \quad (1)$$

where c_0 is propagation velocity of the longitudinal wave along the rod, and ρ is material density of the rod.

Dynamic compressibility of a soil, as well as of a number of other compressible materials, is characterized by a shock adiabat, which can be represented in the form of a linear relation:

$$D = A + bu \quad (2)$$

Constant A is close to the propagation velocity of a plane compression wave along the soil at low pressures, and b characterizes limiting compressibility of the soil.

It is known that the plane wave propagation velocity in a soil increases with the level of water-saturation, and so does the unloading wave velocity. This results in a smaller duration of the compression pulse in the measuring rod as compared with a wet soil (Kotov, 2016). So, in the case of water-saturated soils, determining the force acting on the striker, using strain pulse values on the surface of the measuring rod, becomes problematic due to the distortion of the pulse form because of the dispersion in the process of its propagation along the measuring rod, which was noted earlier by H. Kolsky, R. Davis and other authors (Gorham, 1983; Follansbee, 1983; Tyas, 2014).

Experimental Conditions

The experiments were conducted with a sandy mixture of a natural composition, from which particles of bigger than 1mm and smaller than 0.1mm were removed. The launched containers were filled with dry sand, which was then slightly compacted. The containers were weighted to determine the density of the dry sand and then were filled with a certain amount of water up to the full saturation. Then the containers were weighted again to determine the density of the water-saturated sand and its humidity relative to its initial density. Average density of the initial dry sand and of the water-saturated natural mixture were 1750 kG/m^3 and 2090 kG/m^3 , respectively. The sand consists mainly of quarts particles with the of 2650 kG/m^3 , thus, porosity of the sand is 0.34. When these cavities are completely filled with water, density of the wet sand must increase by 340 kG/m^3 , and the density of the water-saturated sand must be equal to 2090 kG/m^3 , which was practically the case in the preparation of the experiments.

The 0.0205 m -dia steel measuring rod was 1.5 m -long; the density of the rod material was $\rho = 8050 \text{ kG/m}^3$, Young modulus was $E = 186 \text{ GPa}$, yield strength was 2 GPa , wave propagation velocity along the rod was $c_0 = \sqrt{E/\rho} = 4807 \text{ m/s}$.

Fig.2 shows time histories of resistance to penetration of a flat-nosed striker into a dry (curves 1, 2) and a water-saturated (curves 3, 4) sandy soil at impact velocities of 182 and 192 m/s, respectively, as observed in inverse experiments. The experimental data correspond to the readings of the strain gages cemented to the surface of the measuring rod at a distance of 0.46 m and 0.96 m from the impacted end. The time histories are displaced along the time axis to be clearly discerned.

The data depicted in Fig. 2 clearly shows the effect of geometrical dispersion during the propagation of a strain pulse along the measuring rod, which is manifested in decreasing the amplitude and steepness of the pulse front, increasing its duration and the appearance of oscillations. For the dry sand soil, the dispersion effect is small. In the case of the water-saturated soil, the distortion of the pulse form and the decrease of its maximum value during its propagation along the measuring rod is more pronounced (Kotov,2016).

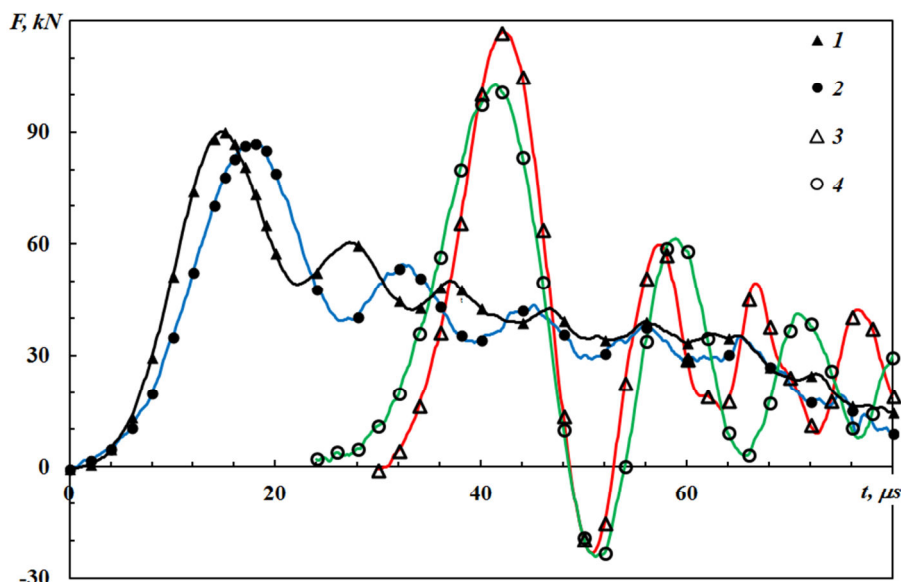


Fig. 2 - Time histories of the penetration resistance force obtained in inverse experiments for penetration velocities of 182 and 192 m/s in a dry and a water-saturated soil, respectively.

Determining the Quasi-Stationary Value of the Resistance Force

In works (Follansbee, 1983; Tyas, 2014; Tyas, 2005) allowances for dispersion were introduced to correct the pulse form, based on the exact solution of Pohhammer-Cree for an infinite elastic cylinder and using Fourier transform. In the experiment, a strain pulse on the surface of the measuring rod is discretely represented as a set of points $e_n = e(t_n)$, $t_n = n\Delta t$, $n = 0, N - 1$, where Δt is discretization step. The dispersion effect for a pulse propagating to a distance of z_0 from the end of the rod results in a frequency displacement of $\Delta\varphi$ in each of the harmonics of the Fourier series (Tyas, 2014)

There also exist modifications of the pulse reconstruction methodologies, based on the exact solution of R. Davis of the problem of propagation of a longitudinal harmonic wave in an elastic circular cylinder, accounting for the non-uniform strain distribution along the cross-section (Tyas, 2005). In this case, Fourier series expansion coefficients are also corrected. By multiplying each harmonic of the Fourier series by M_1 , the strain on the surface of the measuring rod is transformed into an average strain over the cross-section, whereas using multiplier M_2 makes it possible to compute average pressure (Tyas, 2005).

Earlier, to verify the pulse form correction methodology used, the dynamic process of the impact pulse formation was numerically modeled using a modified Godunov method and its propagation along the measuring rod using the “cross” scheme, accounting for its axial symmetry in a formulation corresponding to the inverse experiment (Kotov,2016).

Consider one of the results of an inverse experiment, in which a container with water-saturated soil impacts the flat end of the measuring rod at a velocity of $V_0=320 \text{ m/s}$. The pressures on the contact surfaces of the rod and the soil at the moment of impact are equal, which, taking into consideration (1), (2), makes it possible to obtain an equation for determining mass velocity u , corresponding to impact velocity V_0 : $\rho c(V_0 - u) = \rho_0(A + bu)u$, where c is distribution velocity of a longitudinal wave in a half-space ($c = 5600 \text{ m/s}$); thus, the values of velocity $u = 283 \text{ m/s}$ and maximum stress 1.4 GPa are found. The corresponding maximum value of the force acting upon the front end of the rod is 450 kN .

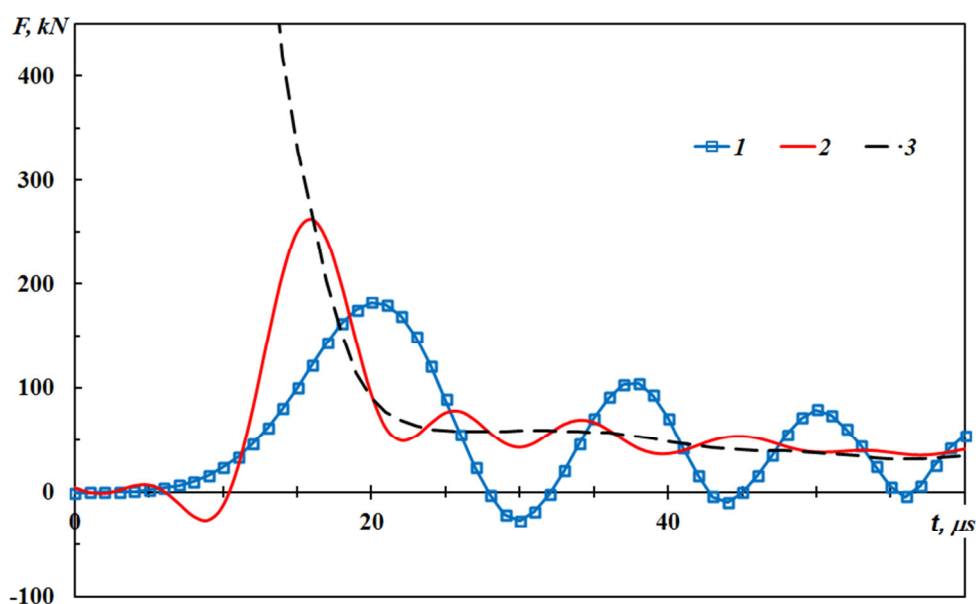


Fig. 3 - Force pulses corresponding to the strain on the surface of the measuring rod, as obtained in an inverse experiment (curves 1 and 2) and computationally (curve 3).

Fig. 3 depicts resistance forces to penetration of a striker into a water-saturated soil at a velocity of 320 m/s . Curve 1 corresponds to force $F = Ee(t)S_0$, where strain pulse $e(t)$ is registered on the surface of the measuring bar at a distance of 0.96 m from its end; curve 2 represents experimental data with the account of dispersion and of the non-uniform strain distribution over the cross-section of the rod according to formulas (2); curve 3 shows the results of computations. For a more vivid presentation, the pulses are displaced along the time axis to the origin of the coordinates.

Proximity of the numerical and experimental results at the quasi-stationary stage of penetration and substantial difference in the maximum values are noted.

Fig. 4 presents the amplitude-frequency characteristic of strain pulse ($f = \omega/(2\pi)$) propagating along the rod. Curves 1 and 2 correspond to the experimental and computational results for a pulse at a distance of 0.96 m from the bar end, curve 3 represents the specter of the computed pulse at the bar end (curve 3 in Fig. 3). It is to be noted that for the frequency of over $f_k = 140 \text{ kHz}$ the amplitude of the pulse propagating along the rod drops to zero, whereas the initial pulse amplitude at the bar end is non-zero.

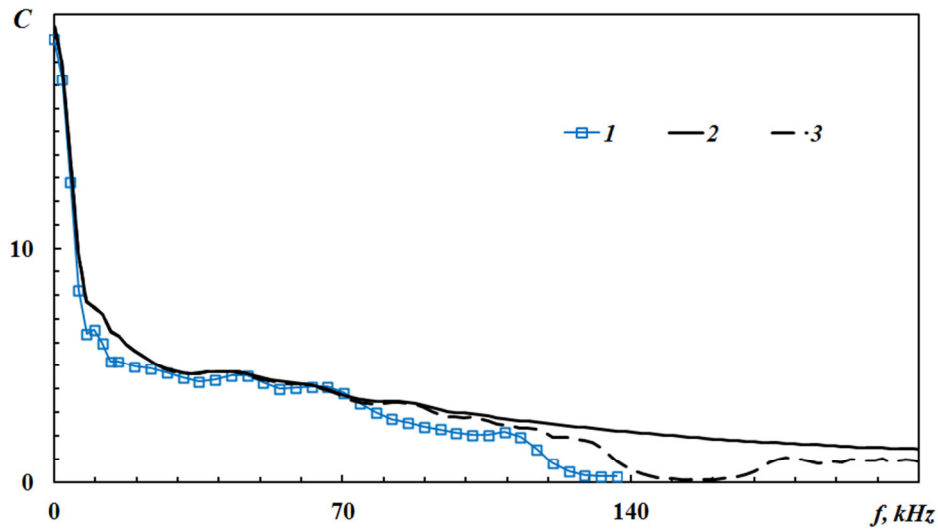


Fig. 4 - Amplitude-frequency characteristics of the pulses in the measuring rod

The above frequency, as was earlier noted in (Kotov, 2016; Gorham, 1983; Follansbee, 1983; Tyas, 2014; Tyas, 2005; Balandin VI.VI, 2016), is critical for a rod of the given radius. Thus, the employed pulse form correction procedure does not make it possible to determine the maximum of such a short pulse, however, the resistance force value at the quasi-stationary stage of penetration, settling after an abrupt drop, is determined fairly accurately.

NUMERICALLY MODELING PROCESSES OF IMPACT AND PENETRATION INTO WATER-SATURATED SOIL

Approximation of the Shock Adiat of the Soil

The representation of the shock adiabat (2) in the form of linear relation $D(u)$ using Hugoniot relations $\sigma = \rho_0 Du$, $\theta = u/D$ can be transformed into $\sigma(\theta) = \rho_0 A^2 \theta / (1 - b\theta)^2$, $\theta = 1 - \rho_0 / \rho$, where $\sigma(\theta)$ is stress as a function of volumetric strain, ρ_0 and ρ are initial and current soil density.

To conduct strength analyses of a soil mixture in a wide parameter range, the following equation of state of a model of a multi-component medium can be used as a fairly accurate approximation of the shock adiabat:

$$\frac{\rho_0}{\rho} = \sum_{i=1}^3 \alpha_i \left(\frac{\sigma}{B_i} + 1 \right)^{\frac{1}{n_i}}, \quad B_i = \frac{\rho_{i0} c_{i0}^2}{n_i}, \quad i = 1, 2, 3 \quad (3)$$

where $\alpha_1, \alpha_2, \alpha_3$ are volume concentrations of free porosity (pinched air and/or other gases), liquid (water) and quartz; ρ_{i0} and c_{i0} , $i = 1, 2, 3$ are densities and propagation velocities of the longitudinal waves in the corresponding components, ρ , σ are density and mixture pressure, ρ_0 are initial values, $\rho_0 = \alpha_1 \rho_{10} + \alpha_2 \rho_{20} + \alpha_3 \rho_{30}$, $\alpha_1 + \alpha_2 + \alpha_3 = 1$

the known values of the constants from equation (3), pertaining to the shock adiabat parameters of water and quartz, are listed in the following table:

Table 1 - Shock adiabat parameters of water and quartz

i	$\rho_{i0}, kG/m^3$	B_i, MPa	n_i	$c_{i0}, m/s$
2	1000	304.5	7.15	1475
3	2650	9118.7	4	3710

Values ρ_{i0} , B_i , n_i , corresponding to the compressibility of initial free porosity, are not related with the compressibility of the gas component and are experimentally determined for each soil in particular.

Earlier, results were obtained (Balandin, 2015a) in plane-wave experiments with sand specimens with the particle sizes of 0.2-0.315 mm in the velocity range of 100 - 500 m/s, where shear properties of sandy soil are considerable. The density of dry sand was $1600 \pm 50 kG/m^3$, the density of water-saturated sand was $1900 \pm 50 kG/m^3$.

The parameters of state equation (3) for the dry and wet soils were as follows: the value of free space density was taken to be equal to the density of air $\rho_{i0}=1.300 kG/m^3$, whereas parameters B_i and n_i were chosen using the least square method as those which provide the best agreement with the experimental results for the dry soil. Humidity of the soil was determined using the following formula: $w = \frac{\rho_0 - \alpha_3 \rho_{30}}{\alpha_3 \rho_{30}} \cdot 100\%$.

In (Balandin, 2016), maximum resistance force as a function of impact velocity $F(V_0)$ were obtained for the interaction of a sandy soil of average density $\rho_0=1725 kG/m^3$ and $w=0.1\%$, with a cylindrical rod with a flat front end; in the same work, shock adiabat constants (1) $A=455 m/s$, $b=2.25$ were determined (Balandin, 2016).

For the parameter values of a three-component mixture of $\alpha_1=0.3486$, $\alpha_2=0.001$, $\alpha_3=0.6504$, initial density $\rho_0=1725 kG/m^3$ and soil humidity $w=0.1\%$, the value of the constants of equation (3), corresponding to the porous component, were determined as: $B_1=103 MPa$ and $n_1=1.4$. For a soil with humidity $w=18\%$ and initial density $\rho_0=2035 kG/m^3$, the values of the parameters of equation (3) were found as: $\alpha_1=0.0396$, $\alpha_2=0.31$, $\alpha_3=0.6504$.

Shock adiabat constants (1) were obtained based on three-component equation (3) for mass velocity u changing in the range of 50 to 350 m/s and for soils of various humidity values, as summarized in the following table 2:

 Table 2 - Shock adiabat constants $D(u)$ of the water-containing soil

№	$w, \%$	$\rho_0, kG/m^3$	$A, m/s$	b
1	0.1	1725	455	2.25
2	10	1895	645	3.2
3	18	2035	1290	3.6
4	20	2075	1700	3.5

Numerical modeling methodology

The computations were done using the “Dinamika-2” software complex (Abuzyarov, 2000; Bazhenov, 2002), implementing Grigoryan’s mathematical model of the dynamics of elastoplastic soil media. The main relations of the model are written in a cylindrical coordinate system as a set of differential equations expressing laws of conservation of mass, pulse, and maximal density reached in the process of actively loading the soil, as well as equations of plastic flow with Mizes plasticity condition

$$d\rho/dt + \rho(u_{r,r} + u_{z,z}) = -(\rho u_r)/r,$$

$$\rho du_r/dt - \sigma_{rr,r} - \sigma_{rz,z} = (\sigma_{rr} - \sigma_{\theta\theta})/r,$$

$$\rho du_z/dt - \sigma_{rz,r} - \sigma_{zz,z} = (\sigma_{rz})/r,$$

$$d\rho^*/dt = d\rho/dt H(\rho - \rho^*) H(d\rho/dt),$$

$$D_J s_{ij} + \lambda s_{ij} = 2G e_{ij}, \quad (i, j = r, z),$$

$$s_{ij} s^{ij} \leq \frac{2}{3} \sigma_T^2,$$

where t is time, ρ and ρ^* are initial, current and maximal density reached in the loading process, u_i , σ_{ij} , s_{ij} , e_{ij} are components of the velocity vector, of Cauchy stress tensor and of deviators of stress tensors and strain rates, p is pressure, H is Heaviside function, D_J is Yauman derivative, d/dt is complete time derivative, G is shear modulus, σ_T is yield strength, with the summation over the repeated indices. Parameter $\lambda = 0$ for elastic deformation, but $\lambda > 0$, if the plasticity condition is realized.

The system is closed with finite relations (Bazhenov, 2003), determining dynamic compressibility $p = f_1(\rho, \rho^*) H(\rho^* - \rho) H(\rho_0 - \rho)$ and shear resistance of the soil medium $\sigma_T = f_2(p)$, where ρ_0 is initial density.

The striker is assumed non-deformable, moving as a rigid body normally to the free surface of the soil at a constant velocity (the formulation is close to that implemented in the inverse experiment). The value of resistance force to the penetration of the striker F at each time step of the analysis is calculated by integrating the stresses at the wetted surface of the striker. $F = \iint_S [\sigma_n \mathbf{n} + \sigma_\tau \boldsymbol{\tau}] dS$, where σ_n and σ_τ are normal and tangential stresses, \mathbf{n} and $\boldsymbol{\tau}$ are unit vectors of the internal normal and a tangent in the body surface element.

Changing of the contact surface in time is accounted for using the contact algorithm of “impenetrability” along the normal with “the sliding along the tangent with dry friction”

$$\dot{u}'_s = \dot{u}''_s, q'_s = -q''_s, q_s = q'_s = \begin{cases} q_s, & |q_s| \leq k |q_\xi| \\ k |q_\xi| \cdot \text{sign}(q_s), & |q_s| > k |q_\xi| \end{cases}$$

where \dot{u}_α , q_α are components of the vectors of displacement velocity and of contact pressure in a local coordinate basis ($\alpha = s, \xi$), s is direction of the tangent, ξ are normals; k is sliding friction coefficient; signs ' and '' indicate the corresponding values on the opposite

sides of the contact. The equation set of the dynamics of the soil medium is completed with initial and boundary conditions.

RESULTS

Resistance to shear can be described by a fractionally rational dependence of the yielding of the soil on pressure $\sigma(p) = f_2(p) \equiv kp/(1 + kp/Y)$, where k is internal friction coefficient, Y is maximal yield strength; the cohesion value can be neglected for this kind of soil. The relation between pressure and volumetric strain (density), required for the analysis is assumed in the form of $p(\theta) = f_1(\theta) \equiv \rho_0 a^2 \theta / (1 - b\theta)^2$, where $a = A/\sqrt{1 + 2k/3}$ (Balandin, 2015a).

To determine parameters of the dependence of yield strength on the pressure of a water-saturated soil, an experimental-computational method (12). Based on the results of a series of computations, the following parameter values of the state equation of water-saturated sand were obtained: $A=1300 \text{ m/s}$, $b=3.6$, $k=0.5$, $Y=50 \text{ MPa}$. For dry sand, the following values were earlier obtained: $A=455 \text{ m/s}$, $b=2.25$, $k=1.2$ and $Y=300 \text{ MPa}$ (Balandin, 2016).

In what follows, the results of numerically analyzing the penetration of a flat-nosed cylindrical striker into a water-saturated sandy soil in an elastoplastic formulation are given. Surface friction was not accounted for in the numerical computations, as there is practically no displacement of soil particles along the flat end of the striker-rod, whereas the flow of the soil over the cylindrical part adjacent to the end of the striker is of a cavitation character.

The above results are compared with the computational results in a hydrodynamic formulation, where a soil is described using a model of a nonlinear compressible liquid with the same shock adiabat but in the complete absence of shear resistance ($k = Y = 0$, $a = A$).

Fig. 5 shows the values of resistance force at a quasi-stationary penetration stage as a function of mass velocity u . The dark and the light boxes represent the data of the inverse experiments; the solid and dotted lines correspond to the results of numerical analysis of the penetration of the striker into dry and water-saturated sands (lines 1 and 3 in Table 2).

The penetration of a striker with a hemispherical nose into a water-saturated sandy soil at a constant velocity was also numerically analyzed. Grigoryan's model of soil media was used in the computations, with the parameters determined from inverse experiments with a flat end. The computations were done using Coulomb friction model with a friction coefficient of 0.2.

Fig. 6 presents time histories of the force of resistance to penetration of a striker at a velocity of $V_0=282 \text{ m/s}$. The light boxes correspond to the results of the inverse experiment, the dotted and the dashed lines depict the computational results, accounting for the shear properties and in a hydrodynamic formulation, respectively.

Also compared were experimental and numerically computed maximum values of the force of resistance to penetration of a striker with a hemispherical nose into water-saturated sand as a function of impact velocity. In Fig. 6 the dots represent the experimental data (Balandin, 2015b), whereas the dashed and dotted lines correspond to the results of numerical computations, accounting for the shear properties of the soil and in a hydrodynamic formulation (similar to the designations in Figs.5, 6).

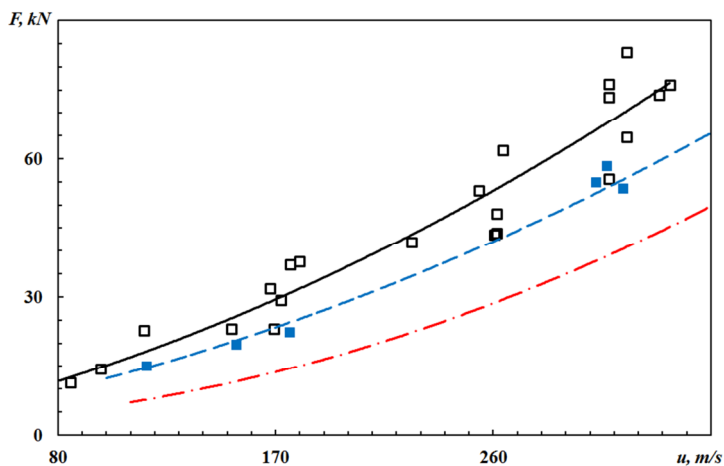


Fig. 5 - Values of the penetration resistance force at a quasi-stationary stage of the penetration of a flat-nosed striker into the water-saturated sandy soil (experimental and computational)

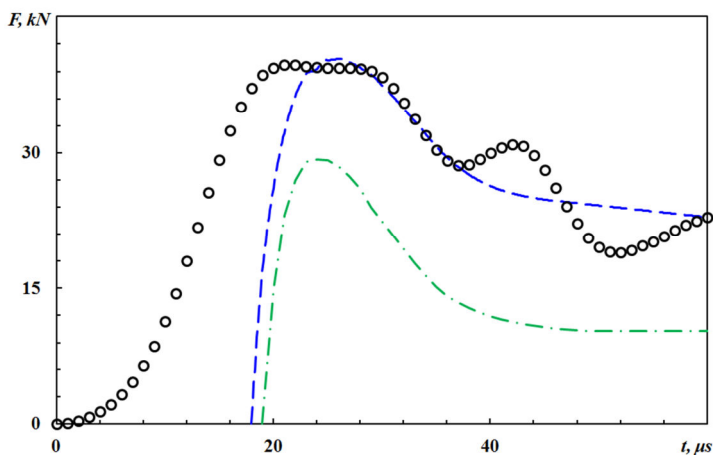


Fig. 6 - The dependence of the resistance force to penetration of a striker with a hemispherical nose into the water-saturated sandy soil at a velocity of 282 m/s (experimental and computational)

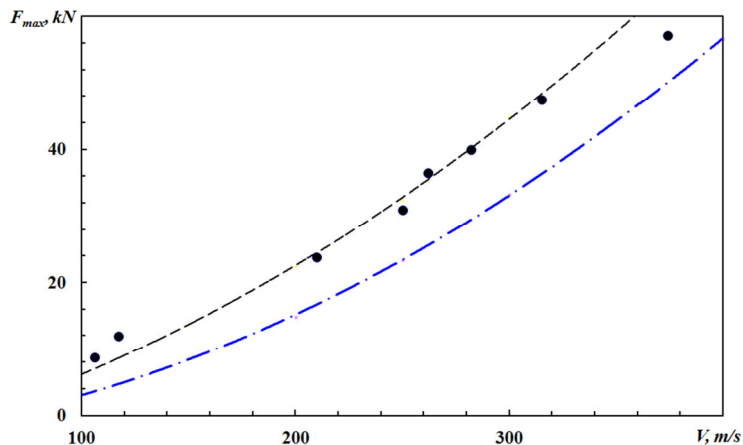


Fig. 7 - Maximum force of resistance to penetration of a hemisphere into water-saturated sand as a function of the impact velocity (the dots represent the experiment, the lines show the computed values)

CONCLUSION

It is evident in Figs. 4-6 that both maximum and quasi-stationary values of the forces of resistance to penetration of strikers with a flat and a hemispherical front end into a soil, obtained experimentally, are close to the computed values with the account of the shear properties in the framework of the model of a compressible elastoplastic medium. The computational results in the hydrodynamic formulation considerably differ from the experimental ones. It was shown earlier (13) that the maximal and the quasi-stationary value of the force resistance to penetration of a hemispherical striker are mainly determined by the values of the internal and surface friction coefficients, whereas the effect of the shock adiabat on the force characteristics of the penetration process is considerably less pronounced.

Thus, when compacted sand is almost fully water-saturated, its shear properties degrade, but remain considerable enough to be taken into account. The obtained results will be useful in analyzing loads acting on the front parts of solid deformable bodies penetrating into water-containing soils.

ACKNOWLEDGMENTS

The work was done with financial support from RFFI (Grants №№16-08-00825, 15-08-7977, 16-01-0524).

REFERENCES

- Abuzyarov M.Kh, Bazhenov V.G., Kotov V.L., Kochetkov A.V., Krylov S.V., Fel'Dgun V.R. A Godunov-type method in dynamics of elastoplastic media. *Computational Mathematics and Mathematical Physics*, 2000, 40(6), p. 900-913.
- Arlery M., Gardou M., Fleureau J.M., Mariotti C. Dynamic behaviour of dry and water-saturated sand under planar shock conditions. *International Journal of Impact Engineering*, 2010, 37, p. 1-10,
- Balandin V.V., Balandin V.I., Bragov A.M., Krylov S.V., Tsvetkova E.V. Experimental and theoretical study of penetration of spherical solids into wet sand. *Journal of Applied Mechanics and Technical Physics*, 2015, 56(6), p. 972-976.
- Balandin V.V., Bragov A.M., Igumnov L.A., Konstantinov A.Yu., Kotov V.L., Lomunov A.K.: Dynamic Deformation of Soft Soil Media: Experimental Studies and Mathematical Modeling. *Mechanics of Solids*, 2015, 50(3), p. 286-293.
- Balandin V.I., Balandin V.I., Bragov A.M., Kotov V.L.: Experimental Study of the Dynamics of Penetration of a Solid Body into a Soil Medium. *Technical Physics*, 2016, 61(6), p. 860-868.
- Balandin V.I., Kotov V.L. Studying the propagation of a stress pulse in an elastic cylindrical bar, *Problems of Strength and Plasticity*, 2016, 78 (4), p. 388-395, (in Russian)
- Bazhenov V.G., Bragov A.M., Kotov V.L., Kochetkov A.V. An Investigation of the Impact and Penetration of Solids of Revolution into Soft Earth. *J. Appl. Math. Mech.*, 2003, 67(4), p. 611-620.
- Bazhenov V.G., Bragov A.M., Kotov V.L.: Experimental-Theoretical Study of the Penetration of Rigid Projectiles and Identification of Soil Properties. *J. Appl. Mech. Tech. Phys.*, 2009, 50(6), p. 1011-1019.

Bazhenov V.G., Kotov V. L. Method for Identifying Elastoplastic Properties of Ground Media by Penetration of Impactors. *Mech. Solids.*, 2008, 43(4), p. 678-686.

Bazhenov V.G., Kotov V.L. Modification of Godunov's numerical scheme for solving problems of pulsed loading of soft soils. *Journal of Applied Mechanics and Technical Physics*, 2002, 43(4), p. 603-611.

Bragov A.M., Balandin V. V., Lomunov A.K., Filippov A.R.: Determining the Impact Compressibility of Soft Soils from Reversed Test Results. *Tech. Phys. Lett.*, 2006, 32(6), p. 487-488.

Bragov A.M., Grushevskii G.M. Influence of the Moisture Content and Granulometric Composition on the Shock Compressibility of Sand. *Tech. Phys. Lett.*, 1993, 19, p. 385-386.

Bragov A.M., Grushevsky G.M., Lomunov A.K. Use of the Kolsky Method for Confined Tests of Soft Soils. *Exper. Mech.*, 1996, 36(3), p. 237-242.

Bragov A.M., Kotov V.L., Lomunov A.K., Sergeichev I.V. Measurement of the dynamic characteristics of soft soils using the kolsky method. *Journal of Applied Mechanics and Technical Physics*, 2004, 45(4), p. 580-585.

Dianov M. D., Zlatin N. A., Mochalov S. M., et al. Shock Compressibility of Dry and Water-Saturated Sand. *Sov. Tech. Phys. Lett.*, 1977, 2, p. 207-208.

Follansbee P.S., Frantz C. Wave propagation in the split Hopkinson pressure bar. *Journal of Engineering Materials and Technology*, 1983, 105(1), p. 61-66.

Gorham D. A numerical method for the correction of dispersion in pressure bar signals. *Journal of Physics E: Scientific Instruments*, 1983, 16, p. 477-479.

Kotov V.L., Balandin V.I., Balandin V.I.: Investigation of applicability of reversed experiment techniques to determine the dynamic characteristics of saturated soils. *PNRPU Mechanics Bulletin*, 2016, (3), p. 97-107

Kotov V.L., Balandin V.I., Bragov A.M., Balandin V.I. Quasi-steady motion of a solid in a loose soil with developed cavitation. *Doklady physics*, 2013, 58(7), p. 309-313. Martin B. E., Chen W., Song B., Akers S.A. Moisture effects on the high strain-rate behavior of sand. *Mechanics of Materials*, 2009, 41, p. 786-798.

Omidvar M., Iskander M., Bless S.: Stress-Strain Behavior of Sand at High Strain Rates. *Int. J. Impact Engng.*, 2012, 49, p. 192-213.

Tyas A, Ozdemir Z.: On backward dispersion correction of Hopkinson pressure bar signals. *Philosophical Transactions of the Royal Society A: Mathematical, Physical and Engineering Sciences*, 2014, 37(2), p. 1-11.

Tyas A, Pope D.J. Full correction of first-mode Pochhammer-Chree dispersion effects in experimental pressure bar signals. *Measurement Science & Technology*, 2005, 16(3), p. 642-652.